# The GNSS NavAer INCT Project Overview and Main Results

João Francisco Galera Monico[1*] iD, Eurico Rodrigues de Paula[2] iD, Alison de Oliveira Moraes[3] iD, Emanoel Costa[4] iD, Milton Hirokazu Shimabukuro[1] iD, Daniele Barroca Marra Alves[5] iD, Jonas Rodrigues de Souza[2] iD, Paulo de Oliveira Camargo[1] iD, Fabricio dos Santos Prol[6] iD, Bruno César Vani[7] iD, Vinicius Stuani Amadeo Pereira[8] iD, Paulo Sergio de Oliveira Junior[9] iD, Italo Tsuchiya[1] iD, Claudinei Rodrigues Aguiar[10] iD

1. Universidade Estadual Paulista Júlio de Mesquita Filho ROR – Faculdade de Ciência e Tecnologia – Departamento de Cartografia – Presidente Prudente/SP – Brazil.
2. Instituto Nacional de Pesquisas Espaciais ROR – Divisão de Heliofísica, Ciências Planetárias e Aeronomia – Ciências Espaciais e Atmosféricas – São José dos Campos/SP – Brazil.
3. Departamento de Ciência e Tecnologia Aeroespacial ROR – Instituto de Aeronáutica e Espaço – São José dos Campos/SP – Brazil.
4. Pontifícia Universidade Católica do Rio de Janeiro ROR – Rio de Janeiro/RJ – Brazil.
5. Universidade Estadual Paulista Júlio de Mesquita Filho ROR – Faculdade de Ciência e Tecnologia – Departamento de Matemática e Computação – Presidente Prudente/SP – Brazil.
6. Finnish Geospatial Research Institute ROR – Department of Navigation and Positioning – Helsinki/Kirkkonummi – Finland.
7. Instituto Federal de Educação Ciência e Tecnologia de São Paulo ROR – Presidente Epitácio/SP – Brazil.
8. Universidade Tecnológica Federal do Paraná ROR – Coordenação de Agronomia – Santa Helena/PR – Brazil.
9. Universidade Federal do Paraná – Departamento de Geomática ROR – Curitiba/PR – Brazil.
10. Universidade Tecnológica Federal do Paraná ROR – Coordenação de Engenharia Civil – Apucarana/PR – Brazil.

*Correspondence author: galera.monico@unesp.br

## ABSTRACT

Air navigation is increasingly dependent on the use of Global Navigation Satellite Systems (GNSS). It allows the determination of the aircraft's position in all phases of the flight and brings many advantages. Although GNSS navigation results in gains, the radio signals from these systems are strongly influenced by the ionospheric environment. It introduces errors that can affect the accuracy, integrity, availability and continuity requirements established by the International Civil Aviation Organization (ICAO). The ionospheric layer has different behaviors depending on the latitude, time of day, season of the year, geomagnetic activity and solar cycle. Since Brazil is located in a region of low latitudes, it experiences a series of unique challenges when compared to regions of mid-latitudes. For this reason, the application of GNSS-based technologies in aviation over the Brazilian territory requires an in-depth assessment of the ionosphere effects. Therefore, the Instituto Nacional de Ciência e Tecnologia (INCT) named GNSS Technology for Supporting Air Navigation was formed in 2017 to better assess the ionosphere impacts and assist government agencies and companies in the development of safe air navigation procedures over Brazil in a near future. This paper presents the most relevant advances achieved so far within this multidisciplinary project that involves Brazilian research centers and universities.

Keywords: Augmentation Systems; Satellite Navigation; Ionospheric Weather over Low Latitudes.

## INTRODUCTION

The use of Global Navigation Satellite Systems (GNSS) in civil aviation is a worldwide trend for the core technology adopted in the present and future for determining the aircraft position during all flight phases. The use of technology of this nature has many advantages, such as considerable reduction in ground support equipment, optimization of the airspace and routes, reduced flight time and consequent fuel savings, among others. In this context, augmentation systems stand out. This technology uses GNSS, especially the North American Global Positioning System (GPS), through the transmission of corrections to improve accuracy in determining position, aiming at conducting aircrafts for precision landings. However, signals from the GPS constellation, as well as those from any other satellite positioning system, are strongly influenced by the ionospheric layer, with the introduction of errors that can compromise the system ability to meet the accuracy, integrity, availability and continuity required by the International Civil Aviation Organization (ICAO). The main aspects of the Ground-Based Augmentation System (GBAS), including the efforts toward its operation in Brazil during the last decade and the prospects for this kind of technology, has recently been reviewed by Marini-Pereira *et al.* (2021a).

The ionospheric layer presents different behaviors, depending on the position, time of day, the season of the year, and the solar activity, with a quasiperiodic behavior of nearly eleven years. The equatorial and low-latitude ionosphere over the Brazilian territory, especially in the regions where the Equatorial Ionization Anomaly (EIA) occurs, has unique characteristics in relation to the rest of the planet. This is due to the concentration of ionospheric phenomena and anomalies that occur over the territory, making the performance of satellite positioning systems in the region worse when compared to mid-latitude regions such as the United States of America and Europe, for example (Abdu *et al.* 2005). For this reason, the application of augmentation systems for GNSS-based technologies in aviation over the Brazilian territory requires a thorough assessment of the effects of the ionosphere (Sousasantos *et al.* 2021). Studies in this sense are of great importance, due to the strict safety requirements involved in aviation, since it involves risks to human lives. Considering this environment, the Instituto Nacional de Ciência e Tecnologia (INCT) named GNSS Technology to Support Air Navigation (GNSS NavAer) was formed in 2017 to carry out a detailed analysis of the ionospheric effects on air navigation use of GNSS.

To achieve this goal, a multidisciplinary group was created under the leadership of the Universidade Estadual Paulista (Unesp) in Presidente Prudente, who has developed research work involving Geodesy, Meteorology and Aeronomy, with the participation of the National Institute for Space Research (INPE), specialized in ionospheric physics studies; Centro de Estudos em Telecomunicações da Universidade Católica/Pontifícia Universidade Católica do Rio de Janeiro (CETUC/PUC-Rio), with extensive experience in telecommunication system; Instituto de Aeronáutica e Espaço (IAE), that has knowledge in aerospace systems and aeronautical communications; Instituto Tecnológico de Aeronáutica (ITA), containing contributions in navigation and signal processing; Instituto Federal de São Paulo (IFSP) and Universidade Tecnológica Federal do Paraná (UFTPR), with complementing efforts in various related subjects. The main aim of this INCT has been to fulfil the demands from the Brazilian society to specifically ensure safe GNSS-based air navigation.

Among the several efforts of this project, the following aspects should be listed: the expansion of the Brazilian network of scintillation monitors; a solid and complete assessment of the ionospheric dynamics over Brazil; an evaluation of the ionospheric effects on augmentation system operations; the development of an ionospheric threat model for GBAS operations in Brazil; a statistical modeling of ionospheric scintillation; research on new GNSS positioning techniques; investigation on the receiver performance improvement under scintillation; and human resource training.

One of the main motivations of the project is the analysis of the ionospheric threat model, developed for use in the United States of America, which guarantees the safe operation of precision landing systems such as the GBAS. However, a feasibility analysis for the use of this model in Brazil is required. Indeed, the Brazilian ionospheric conditions are quite different from those under which the original model was developed. Changes and improvements to this threat model have been developed to adapt it to the Brazilian reality and to meet the criteria required by ICAO. During the development of the project, a consistent and comprehensive data set from GNSS receivers in the national territory has been used to support the analysis of the specificities of the Brazilian ionosphere and the consequent viability of the use of GNSS technologies for air navigation. For this reason, the

existing continuous monitoring networks have been expanded, as well as the main data access interface of this network, the Ionospheric Scintillation Monitoring Receiver (ISMR) Query Tool described by Vani *et al.* (2017), which is a web-based software and has been updated. These networks are composed of GNSS receivers capable of measuring the most important parameters which indicate ionospheric activity: Total Electronic Content (TEC) and ionospheric amplitude and phase scintillation indices $S_4$ and $\sigma_\phi$, respectively. These indices estimate the standard deviation of the: (1) normalized received power I/<I> (where <I> is the average value of the received power I); and (2) phase fluctuations.

The above demand was presented by the Departamento de Controle do Espaço Aéreo (DECEA) to serve the Brazilian community with a safe service for precision landing procedures. The data from GNSS receivers of these networks have been used to optimize the performance of GNSS receivers during the occurrence of ionospheric scintillation, and to provide users with real-time maps of the errors caused by the ionospheric delay and the occurrence of scintillation. Such maps are useful in several geodetic applications, including precision agriculture and positioning of oil prospecting platforms. They can also be assimilated by ionospheric models and used in several scientific studies. It is also envisaged that, in the future, the total electron contents (TEC) and scintillation maps will be incorporated to another service provided by the Sistema de Controle do Espaço Aéreo Brasileiro (SISCEAB).

The INCT is a vector responsible not only for research, but also for the generation of human resources for the aeronautical industry sector. It is worth mentioning that it results in the construction and establishment, in the country, of technical, scientific and technological competences in the areas of electronic and aerospace engineering. The mastery of positioning and navigation satellite technologies as well as the continuous training of professionals, whether in research or innovation in the productive sector, appears as important steps for the effective strengthening of public policies in Brazil.

The main objective of this paper is to present the latest advances provided by the GNSS NavAer INCT project associated with ionospheric effects on GNSS signal and positioning, as well as the proposed methodologies to mitigate these effects. It should be mentioned that the reader can find many other contributions that are still in progress in https://inct-gnss-navaer.fct.unesp.br.

## Ionospheric Dynamics over Brazil

The first work to be described on the characterization of ionospheric dynamics over Brazil analyzed the effects from the magnetic storm that occurred during the period 06–10 September 2017 on scintillation. It was found that, during the beginning of its recovery phase, a strong zonal eastward electric field penetrated the equatorial region, causing a large upward drift that gave rise to strong ionospheric scintillation. It was also observed that, during the night after this effect, the zonal westward electric field inhibited the plasma drift in the equatorial region due to the disturbed dynamo, as well as scintillation. Latitudinal variations in scintillation due to this storm were also analyzed using the GPS frequencies L1, L2C and L5 and larger amplitude and phase amplitudes were observed under the EIA. During the night of 07/08 September 2017, it was also found that the large-scale ionospheric irregularity (Equatorial Plasma Bubble, EPB) reversed its usual movement and drifted from east to west (De Paula *et al.* 2019). Oliveira *et al.* (2020) displayed the TEC maps highlighting the EPB signatures for this storm. Indeed, the left panel of Fig. 1 shows a TEC map for the night 08 September 2017, while the keogram in the right panel presents the zonal plasma drift throughout this night. On 6 September 2017, a X9.3 class solar flare occurred and Pereira *et al.* (2021a) successfully proved that it was possible to use the International GNSS Service (IGS) network infrastructure to detect the event by evaluating an increase in the estimated TEC value.

Souza and Camargo (2019) presented an interesting multi-instrumental study for two distinct nights, with and without records of ionospheric irregularities. Based on ionospheric irregularity indices, ionosonde data and all-sky optical imagers, the authors discussed the potential and limitations of each instrument, and confirmed the benefit of analyzing the ionosphere through the fusion of data from different sensors. Similarly, Oliveira *et al.* (2020) performed a multi-instrumental analysis of the behavior of the ionosphere and proposed a methodology for the construction of TEC maps. Inspired by this work, Marini-Pereira *et al.* (2020) proposed and validated another methodology for TEC map construction. Additionally, they proposed procedures to verify the accuracy of the constructed maps. Their assessment generally showed errors less than 4 m in 99.9% of the cases, even during EPB occurrences.
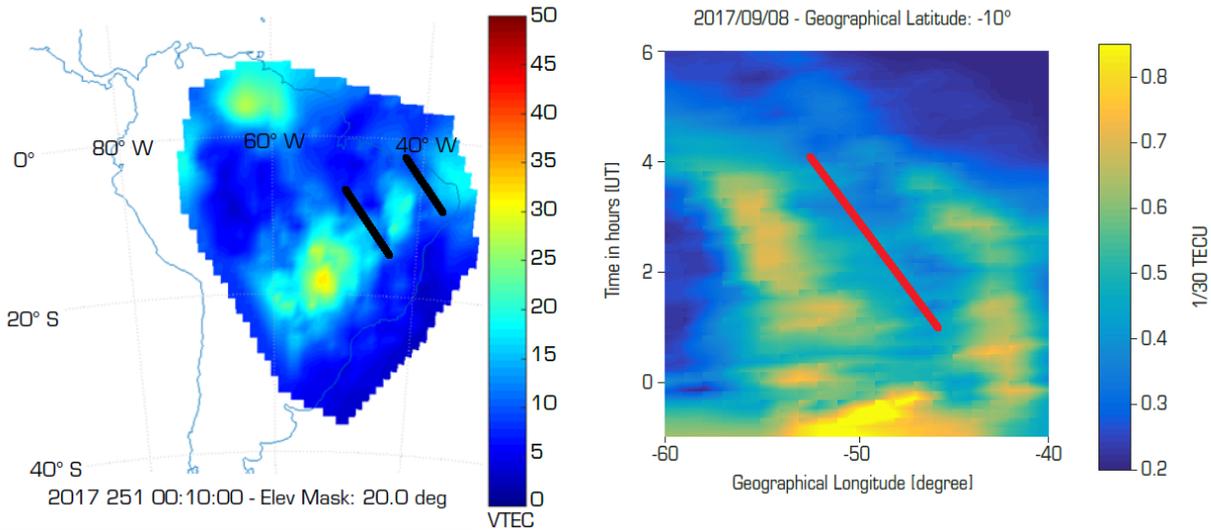
Source: Elaborated by the authors.

**Figure 1.** Left panel: TEC map for 00:10 UTC on 8 September 2017, where the black lines represent EPB structures. Right panel: keogram for the geographic latitude 10° S, showing westward drifts of EPBs.

Another contribution of this project is related to an automatic method to calculate ionospheric plasma bubble zonal drifts from TEC measurements (Silva *et al.* 2019). In fact, pattern recognition was developed to automatically detect EPB structures crossing two GNSS receiving stations. Thus, knowing the distance between the stations and the time for the structure to travel this distance, the drift velocities were obtained. The average results for the EPB zonal velocities estimated by this procedure were in agreement with well-known values. An additional contribution on the same theme was provided by Souza *et al.* (2021), who estimated the EPB zonal drift velocities based on slant TEC measurements from nearby GNSS station pairs. The results obtained by this method were compatible with others available in the literature. A cross-validation showed agreement between estimations based on this technique and the corresponding measurements from other instruments, such as the all-sky image system, for the same events.

An analysis of the climatology of the starting time of ionospheric scintillation in Brazil was carried out under the crests of the EIA. Using data from GPS receivers, it was showed that scintillation occurs approximately 40 min earlier in the months of November and December when compared to January and February. The work suggests that this difference is associated with the magnitude and time of occurrence of the vertical drift prereversal peak of the ionospheric plasma. Based on this climatology, a set of empirical equations has been proposed to alert GNSS users about the occurrence of scintillation (Sousasantos *et al.* 2018).

Another study was developed by Bravo *et al.* (2019). They used the Sheffield University Plasmasphere-Ionosphere Model (SUPIM) INPE to prove that a travelling wave with a velocity equal to 300 m·s⁻¹, propagating from north to south, explains the ionospheric observations at low latitudes in the Brazilian region, during the 29 October 2003 geomagnetic storm.

The ionospheric plasma irregularities are very complex. Their occurrence extends from the E layer up to the top of F region and under favorable conditions, they may occur even in intermediate layers around 150 km height, producing 150 km echoes. Santos *et al.* (2020) explained the dynamics of these ionospheric intermediate descending layers (ILs) over an equatorial and a low-latitude station. The respective stations are São Luís (SL, 2°S; 44°W; magnetic inclination −3.8°) and Cachoeira Paulista (CP, 22.42°S; 45°W; magnetic inclination −34.4°). They found that the occurrence rate of ILs over SL and for the year 2003 is much lower than in 2009, as shown in Fig. 2. This variation does not occur in CP. Figure 2 shows the seasonal occurrence of ILs for the years 2003 (represented by open circles) and 2009 (represented by open triangles) over SL (blue lines) and CP (black lines). The main reason to explain the variation of ILs over SL between 2003 and 2009 is probably due to the increasing displacement of the magnetic equator away from SL during this period.
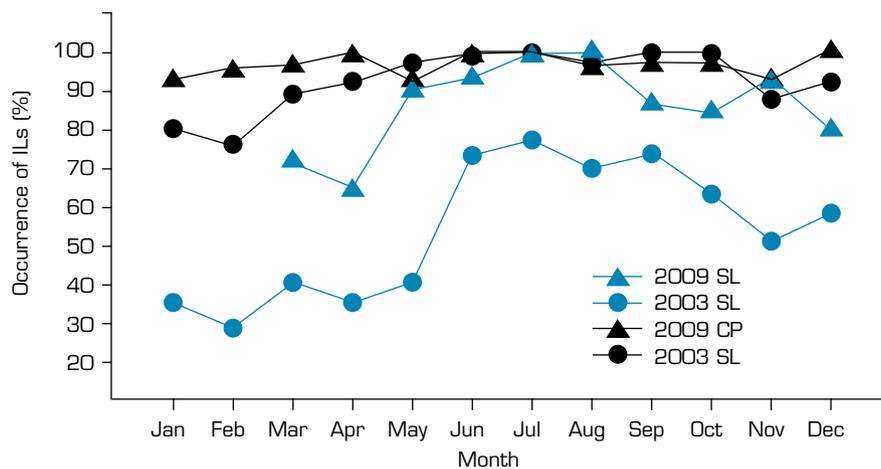
Source: Santos et al. (2020).

**Figure 2.** Percentage of occurrence of intermediate descending layers over São Luís (blue curves) and Cachoeira Paulista (black curves) during 2003 (circles) and 2009 (triangles).

Total Electron Contents suffers substantial changes during solar eclipses. Two studies involving the effects of solar eclipse on the equatorial and low-latitude ionosphere were developed by Bravo *et al.* (2020) and Martínez-Ledesma *et al.* (2020). In the first, the ionospheric response to the total solar eclipse of July 2, 2019 at low latitudes in southern South America was analyzed. Both observations and modeled results showed that the ionospheric layers, below 200 km, decrease with the magnitude of obscuration, as expected. The second study presented a prediction of the ionospheric response to the December 14, 2020 total solar eclipse using SUPIM-INPE model. The prediction revealed the impact of obscuration could produce a decrease in TEC of up to 22%. Decreases of up to 1.5 TECu (1 TECu = $10^{16}$ electrons·m$^{-2}$) could also be observed in the conjugated sector, with respect to the magnetic equator, in South America.

A 20-month statistical evaluation of different TEC estimators was made for the Central and South America regions. Total Electron Contents (TEC) values provided by IGS in the range covered by GNSS monitoring stations were assumed as reference, and were compared with the TEC estimates by the physics-based model (SUPIM) and an empirical model (Neustrelitz TEC Model-Global, NTCM-GL). The discrepancies between SUPIM, NTCM-GL and IGS were caused by the solar flux models used as parametric entries to the models (Klipp *et al.* 2019). It is worth mentioning that the discrepancies in the NTCM-GL results only occur during rapid increases in solar fluxes.

In another work, TEC inferred from Digisonde data were compared with IGS TEC values, which are systematically overestimated by the former ones. The discrepancies were attributed to a limitation in the electron density model for the upper ionosphere plus plasmasphere, adopted to complete the ionogram profiles. It was remodeled using two different approaches: an α-Chapman exponential decay optimization and a corrected version of the NeQuick's formulation (Klipp *et al.* 2020). Both approaches produced coherent and acceptable results. Additionally, Silva *et al.* (2021) compared the following TEC models for the Brazilian sector: Klobuchar, International Reference Ionosphere (IRI-2016) and SAMI2. The IGS TEC from two years around the peak of solar cycle 24 was taken as reference. The results showed that the models presented significant deviations from IGS TEC values, reaching delay of up to 7 m for L1 users under the EIA crest region during the proximity of vertical drift pre-reversal period.

Jesus *et al.* (2020) investigated the occurrence of ionospheric irregularities and scintillation at different latitudes over the South American sector during the high solar activity years of 2013 (F10.7 = 123 solar flux units, sfu) and 2014 (F10.7 = 146 sfu). The index F10.7 measures the solar spectral flux density at the wavelength 10.7 cm in solar flux units (1 sfu = $10^{-22}$ W·m$^{-2}$·Hz$^{-1}$). The parameters TEC, rate of change of the TEC index (ROTI) and the amplitude scintillation index $S_4$ were analyzed. Seasonal variations with maximum occurrence from September to April and little occurrence from May to August were noticed. The investigation also revealed that the longitudinal distances between adjacent EPB structures vary from 600 to 1000 km, which is larger than values reported in several previous studies (Chapagain 2011; Makela *et al.* 2010; Pautet *et al.* 2009; Takahashi *et al.* 2009).

In an effort to characterize the best IGS global ionospheric map (GIM) to be adopted to represent the vertical TEC (VTEC) distribution in Brazil, Jerez *et al.* (2020) have developed a new assessing method using ionosonde data. The method consists in analyzing the correlation between the spatial gradients of VTEC and spatial gradients of the critical frequency at the F2-layer (foF2). Using four years of GIM and ionosonde data, the study has found that the GIM products provided by the Center for Orbit Determination in Europe (CODG) and Universitat Politècnica de Catalunya (UPC), associated to the UPC quarter-of-an-hour time resolution rapid GIM (UQRG), provided the best solutions in the Brazilian region. The results also indicated that the foF2 and VTEC spatial gradients were correlated to the behavior of the ionospheric slab thickness. However, this observation has limitations in the regions with low variability of the slab thickness, as expected.

Prol *et al.* (2018a) analyzed the accuracy of an in-house tomography method to detect and describe plasma depletions associated with EPB. A set of ground-based GNSS receivers, together with electron density profiles derived from GPS radio-occultation measurements, were used in the Brazilian region as input to the developed tomography. The estimated horizontal distribution was compared with simultaneous observations of all-sky images from the 630.0 nm emission line of the atomic oxygen. Figure 3 shows an example of the simultaneous observations of the tomography results and the 630.0 nm emissions for day of year (DOY) 359, 2013 at São João do Cariri (SJCI). This comparison clearly highlights the VTEC depletion aligned with the dark brands of the airglow images, showing the capabilities of tomography. A similar analysis for twenty-three days from 2013 and 2014 obtained a mean rate of success of 25% to 54% for correctly identifying the presence of plasma bubbles by tomography, being more accurate at the geomagnetic equator, where the dimensions of the structures are larger. It was also clear that tomography was capable to map the irregularities even when the meteorological conditions disrupted the possibility of analyzing the OI 630 nm emissions, due to clouds, precipitation, or even due to moonlight brightness contamination. Therefore, tomography was indicated as a useful tool to provide a complementary information to the OI 630 nm emissions in the identification of plasma bubbles. Plasma bubble signatures associated with zonal velocities around 128 to 160 m·s$^{-1}$ were observed.
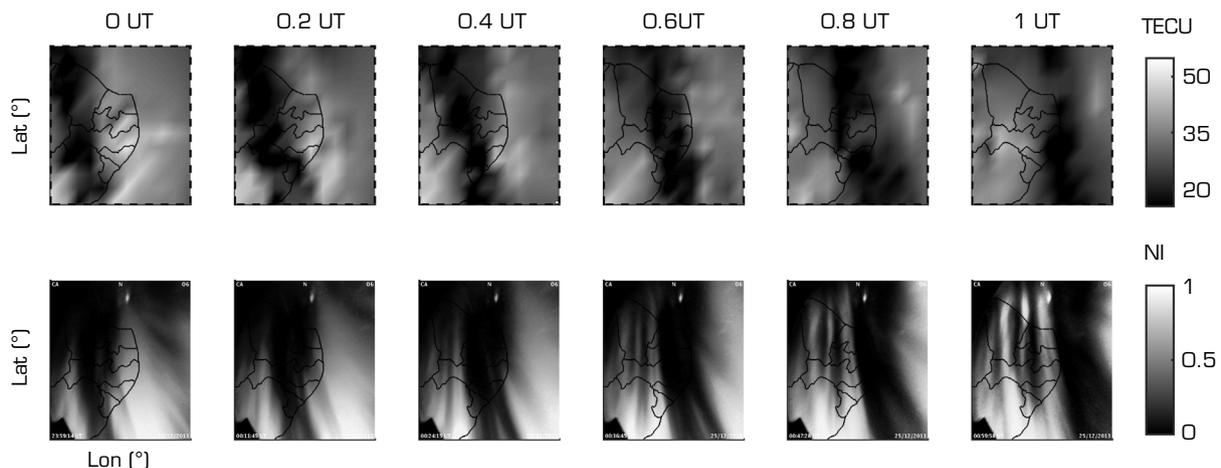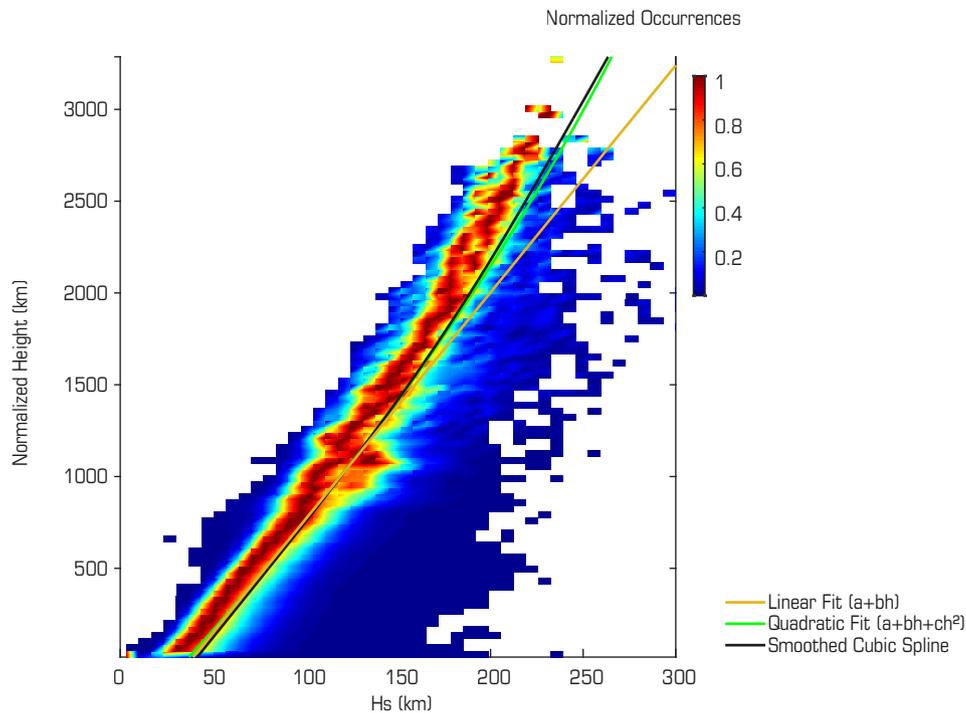


Source: Elaborated by the authors.

**Figure 3.** Example of a plasma bubble drifting through the SJCI region on DOY 359, 2013. The top panels display the plasma depletions by detected tomography and the bottom panels show the co-located results obtained by the all-sky images from the 630.0 nm emission line of the atomic oxygen in units of normalized intensity (NI).

Substantial work has also been done to better understand the topside ionosphere. Prol *et al.* (2018b) has characterized the spatial and temporal patterns of the topside ionosphere using a linear Vary-Chap model and GPS radio-occultation. This investigation has suggested that the equatorial topside was mainly controlled by the equatorial vertical drift, where an evident anticorrelation in the equatorial region was found between the scale height and its first derivative. Indeed, the scale height is higher in the equatorial region due to the direct solar ionization. However, due to the diffusion of the electrons along the geomagnetic field lines, lower values of the gradient of the scale height are observed in the equatorial region. Additionally, the investigation has also found an increase of the gradient of the scale height near 05 local time (LT). This observation was justified by the increase of the

ion production in the topside in response to the solar radiation that first reaches the upper part of this altitude region during the local sunrise. The representation of the topside ionosphere by a linear Vary-Chap is consistent with first principles corresponding to the increase in the electron temperature. However, the altitude where the linear scale height stops to be valid in the topside was not explicitly discussed in the literature until Prol *et al.* (2019a). The investigation has found that the linear behavior of the topside scale height is valid up to 1300 km above the peak height of the F2-layer (hmF2), approximately. Above this altitude, it was found that a quadratic function better describes the topside ionosphere. This is illustrated in Fig. 4, which displays the scale height $H_s(h)$ (that varies with height $h$), a basic parameter of the Vary-Chap model.



Source: Elaborated by the authors.

**Figure 4.** The normalized occurrence shows the height distribution of the scale height $H_s(h)$, a basic parameter of the Vary-Chap model, derived from manually scaled topside electron density profiles of International Satellites for Ionospheric Studies (ISIS) and Alouette missions during the 1960s and 1970s. The solid lines show the linear (brown) and quadratic (green) fitting of the corresponding dataset. A cubic spline fitting (black line), which can be considered a very rigorous fitting approach, is also included. The normalized height $z = (h-h_{mF2})/H_s(h)$ relates to the altitudes above $h_{mF2}$.

## Effects of the Low-Latitude Ionosphere on Augmentation System Operations

Ground-Based Augmentation System is designed to provide service in a local area and to transmit correction messages to aircrafts through ground stations. This system typically includes four single-frequency (L1) GPS reference receivers at precisely known locations, which collect and process pseudorange, carrier phase, power levels and Doppler measurements. These observables are submitted to tests by several quality monitors and the approved outputs are transmitted to an executive monitor for smoothing, corrections and averaging. The resulting differential corrections from the ground system are transmitted to aircrafts via a very high frequency (VHF) data broadcast (VDB) link. The broadcast information includes pseudorange corrections, integrity parameters and various locally relevant data (Marini-Pereira *et al.* 2021a).

Espejo (2020) presented a study of ionospheric effects on a GBAS located under equatorial and low latitude regions. To evaluate the performance of a GBAS, a simulation model of the GPS L1 signal in space was developed, considering ionospheric delay based on statistical distributions of VTEC residuals obtained from IRI-2016 model and estimates using GPS data from Rede Brasileira de Monitoramento Contínuo (RBMC/IBGE) (considering solar and geomagnetic activities, as well as season, local time, and

geomagnetic latitude). The ionospheric delay module is combined with ones for amplitude ionospheric scintillation, simulated based on α–μ probability distributions, and for phase scintillation, generated according to empirical relationships between the indices $S_4$ and $\sigma_\Phi$. The GPS L1 signal model also considers clock and random errors, tropospheric delays, ambiguity, and multipath. Additionally, a statistical analysis of time and spatial ionospheric gradients in the Brazilian region during years with high and low solar and geomagnetic activity was performed, to account for the space decorrelation between GBAS reference receiver and aircraft measurements. The signal-in-space results are injected into a GBAS ground facility simulation model, implemented to detect a varied array of possible anomalies or failures and to generate the differential corrections based on monitoring algorithms. The GBAS performance was evaluated for aircraft approaches under different ionospheric conditions at the Rio de Janeiro and Fortaleza Airports, emphasizing Approach Category I. The horizontal and vertical errors were estimated before any corrections. Next, they are recalculated using GBAS corrections, to evaluate the accuracy improvement. The GBAS integrity is also analyzed, by computing the horizontal and vertical protection levels.

Another contribution to this topic was the work by Marini-Pereira *et al.* (2021b), which evaluated the effectiveness of the use of Satellite-Based Augmentation Systems (SBAS) in the Brazilian territory. Ionospheric error bounds of Grid Ionospheric Vertical Error (GIVE) were generated and presented as maps, considering the geophysical environment. These maps reached values much higher than those found for equatorial and mid-latitude regions. The evaluation showed that SBAS is currently unfeasible for low-latitude regions during EPB periods.

## Development of an Ionospheric Threat Model for GBAS Operation in Brazil

Ground-Based Augmentation System can correct most errors affecting pseudoranges, particularly during periods of nominal ionospheric behavior in the vicinity of an airport. However, depending on the solar flux, geomagnetic activity, local time, season, geographic location and several plasma instability mechanisms and their nonlinear evolutions, the ionosphere can experience severe disturbances, posing potential threats to the integrity of GBAS.

Various researches on GBAS systematic errors due to the ionosphere have been carried out by Lee *et al.* (2007), Pullen *et al.* (2009), and Datta-Barua *et al.* (2010), emphasizing that the subject is important to air navigation and can benefit operators as well as air navigation service providers.

In this way, ionospheric threat models were developed, which determine the maximum ionospheric spatial decorrelation between the GBAS reference stations and the aircraft. For GBAS stations in the Conterminous United States (CONUS) territory, a specific Threat Model is applied. Within this area, the ionosphere is more stable compared to that over Brazil.

The CONUS Threat Model is based on an ionospheric front that moves at a particular horizontal speed, providing ionospheric error gradients (IEG) (Mayer *et al.* 2009). The representation of an ionospheric front and its model parameters are shown in Fig. 5.
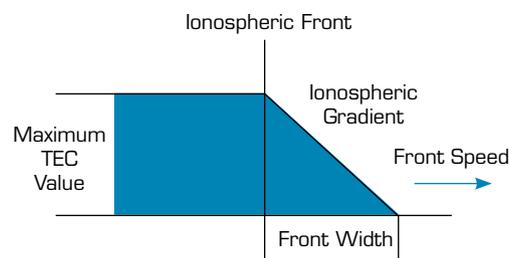
Source: Mayer *et al.* (2009).

**Figure 5.** Representation of an ionospheric front model and its parameters.

The parameter limits are obtained from processing a dataset that includes days with high and low variability in the electronic density of the ionospheric layer. The gradient results are presented as a function of the elevation angle of the satellites, in terms of maximum and minimum values for speed and width and the maximum value of TEC (or ionospheric delay), with no temporal variation for the values.

The methodology for determining the parameters can be found, for example, in Kim *et al.* (2015). To check if the limits of the threat model parameters can be used in a specific region, one of the existing possibilities is using data from a network of GNSS

stations. One of the alternatives for the computation of the gradients is based on the station-pair method, where one of the stations simulates a GBAS and the other an aircraft (Lee *et al.* 2007). Alternatively, the time-step method or the use of GNSS simulators can be used. In the latter case, prior knowledge of the ionospheric conditions in the GBAS region is necessary.

The development of the CONUS Threat Model used 10 days of (L1 and L2) GPS data from Continuously Operating Reference Station (CORS) between the years 2000 and 2004. The limits and variations of the parameters are presented in Table 1 (Datta-Barua *et al.* 2010).

**Table 1.** Limits and variations of CONUS Threat Model parameters. *E* means elevation of the satellite.

| Parameters | Limits and Variations of Parameters (E and IEG) | |
|---|---|---|
| Maximum ionospheric gradient [mm·km⁻¹] | Low Elevation (*E* < 15°) | 375 |
| | Medium Elevation (15° < *E* < 65°) | 375 + 50*(*E* −15°)/50 |
| | High Elevation (*E* > 65°) | 425 |
| Front speed [m·s⁻¹] | 0 – 750 | |
| Front width [km] | 25 – 200 | |
| Maximum ionospheric delay [m] | 50 | |

Source: Datta-Barua *et al.* (2010).

The increasing number of domestic and international flights over Brazil since 2011, concomitantly with the implementation of a Honeywell SLS-4000 GBAS by DECEA at the Rio de Janeiro International Airport for experimental purposes (SBGL, 22°48′S; 43°15′W) inspired studies on ionospheric threat models for Brazil. However, since the navigation aid is certified only for operating in the CONUS region, any other user must estimate the ionospheric parameters of the threat model for the region of intended operation.

Thus, to verify the usability of GBAS in Brazil, 17 RBMC/IBGE stations available within a radius of 500 km from SBGL airport, were selected to estimate the parameters of the corresponding CONUS model for the autumn period (the season most affected by EPBs). In this study, Pereira *et al.* (2021b) used data from 63 days between the years 2000 and 2016 (maximum activities of solar cycles 23 and 24), and a maximum distance of 250 km to form station pairs. Such estimates considered only GPS L1 and L2 carrier-phase measurements and a 10° elevation mask. The ionospheric gradients estimated during the 63 dates as a function of the elevation angles are shown in Fig. 6.
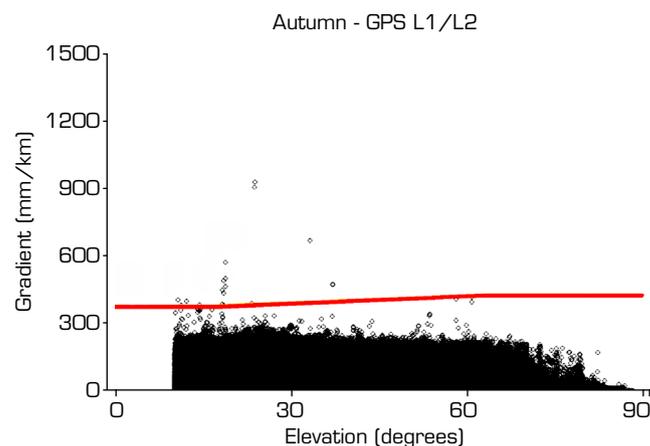


**Figure 6.** Ionospheric gradients as a function of the elevation angles determined from the SBGL airport to GPS satellites. Red line represents the limit of the CONUS Threat Model. Source: Pereira *et al.* (2021b).

Figure 6 indicates that, during the selected autumn days, the estimates exceeding the CONUS Threat Model limits are between elevations 10° and 37°. The gradients that exceeded the limits were less than 930 mm·km⁻¹. Real-time horizontal and vertical protection levels (HPL and VPL) were estimated and compared with the respective horizontal and vertical alert limit (HAL and VAL) values established by ICAO to check the established window. For more details on this research, see Pereira *et al.* (2021b).

## Statistical Modeling of Ionospheric Scintillation

Scintillation models may be used in the estimation of a satellite-based navigation system performance and of the associated positioning errors. Consequently, for scientific and technological developments, ionospheric scintillation modeling is an active research area for the design of new modernized signals and payloads, as well as in the proposition of new applications based on GNSS technology. In this context, a series of researches were carried out to better model and characterize the effect of ionospheric scintillation in Brazil, with emphasis on the modernized signals GPS L2C (1227.60 MHz) and L5 (1176.45 MHz). This section revisits these progresses.

Moraes *et al.* (2018a) statistically analyzed the scintillation environment under a particular condition when the GPS signal propagation paths were aligned with ionospheric plasma bubble structures. Under these circumstances, enhanced scintillation is expected, increasing the occurrence of deep fading, loss-of-lock probability, signal unavailability and positioning errors. Such results of the statistical analysis also showed that this alignment increased the bit error probability and decreased the mean time between cycle slips. The higher occurrence of cycle slips consequently degraded the precise point positioning (PPP) performance, as shown by experiments. Indeed, the PPP results showed a strong influence of high bit error probability values on positioning error, regardless the alignment condition. However, this work also emphasized that high bit error probabilities are more frequent under alignment environments. Figure 7 exemplifies a study case for a receiver at São José dos Campos (23.20°S, 45.85° W, geomagnetic latitude 19.28°S) on the night of 17 November 2014. Extending this study, in Affonso *et al.* (2022), it was evidenced that this alignment condition also causes severe ionospheric gradients that can be threatening for GBAS operation. Their results showed a 10% probability of occurrence of critical gradients exceeding 400 mm·km⁻¹ while nonaligned cases reached only 0.2%.
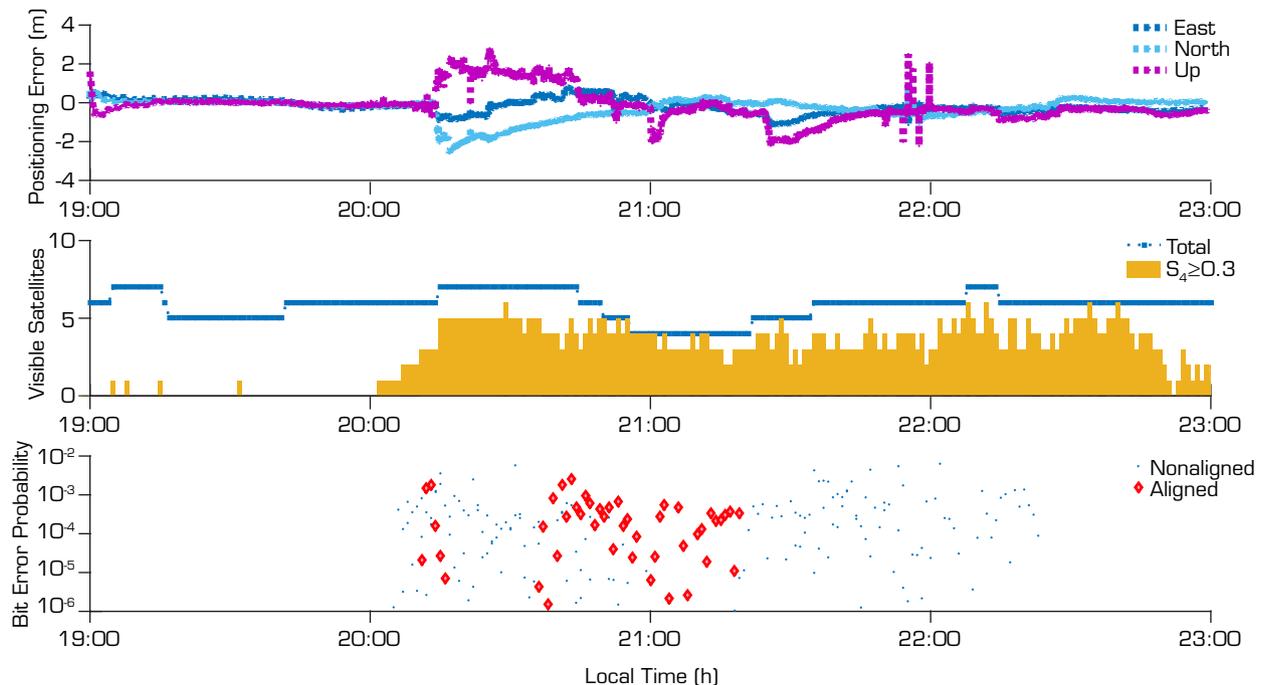
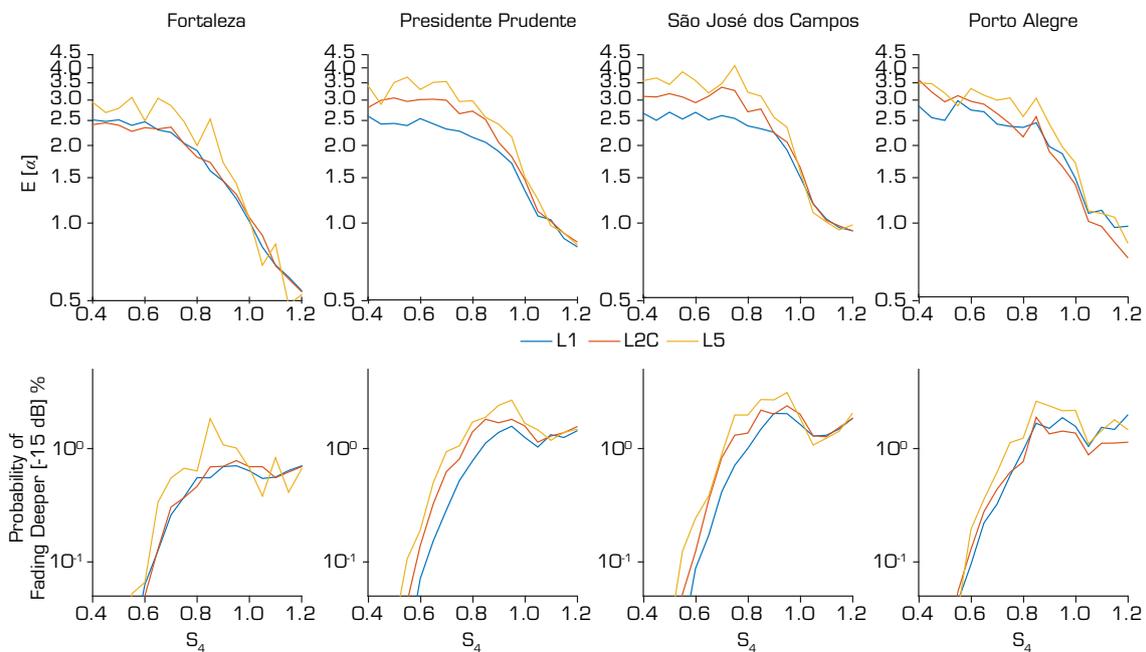

Source: Elaborated by the authors.

**Figure 7.** Example of high bit error probability effects on PPP error, including the particular case of alignment between propagation paths and ionospheric plasma bubble structures.

Another contribution was presented by Moraes *et al.* (2018b), where the statistical distribution of severe fade events was modeled using the α-μ distribution (Yacoub 2007a). The results from the analysis were presented in the form of fading coefficients for distinct scintillation levels, using data from four Brazilian sites. It was evidenced that sites under the EIA crest presented a higher probability of strong fading events, in comparison with the other stations. Another important finding was related to the L5 signal, designed for safety-of-life applications. This particular signal was revealed to be more affected by scintillation when compared to those at other GPS frequencies. A series of fading coefficients were provided and can be used by theoretical works to predict the fading environment that users might expect in similar circumstances. Second-order statistics were validated by Moraes *et al.* (2014a). Figure 8 shows the average α values, based on the empirical measurements, and the respective probability of fading events deeper than –15 dB for different sites characterized in Table 2. Based on the bottom panel values, it is possible to verify that the range between $0.7 < S_4 \leq 0.9$ presented the highest probabilities of fading events deeper than –15 dB. Marini-Pereira *et al.* (2019) proposed and validated a new methodology for estimating the α-μ fading coefficients based on the autocorrelation function of the amplitude scintillation. These coefficients may also be estimated by moment relations (Yacoub 2007a) or the maximum likelihood method as applied in the work of Moraes *et al.* (2019) based on the weighted least squares fit approach of Coleman and Li (1994).

**Table 2.** Site information and available data.

| Station | Latitude | Longitude | Geom. latitude (GMLAT) | Available Data (h) |
|---|---|---|---|---|
| Fortaleza | 3.74°S | 38.57°W | 8.86°S | 695 |
| Presidente Prudente | 22.12°S | 51.40°W | 16.01°S | 665 |
| São José dos Campos | 23.20°S | 45.85°W | 19.28°S | 700 |
| Porto Alegre | 30.07°S | 51.01°W | 22.32°S | 640 |

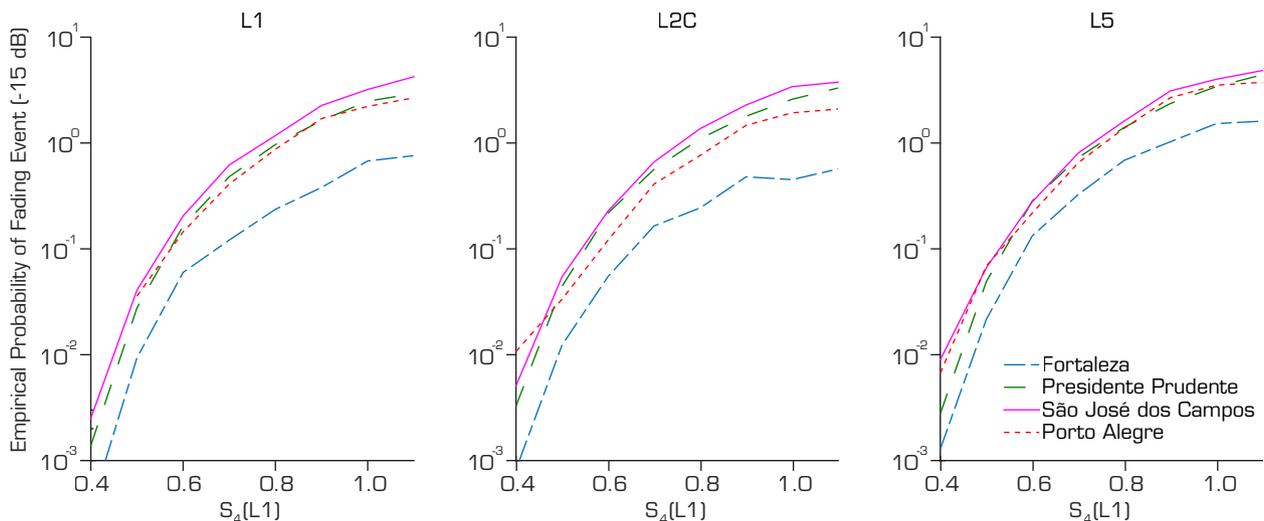Source: Elaborated by the authors.



Source: Elaborated by the authors.

**Figure 8.** The top panels show the average fading coefficient α as a function of the amplitude scintillation index $S_4$ for different sites characterized in Table 2. The bottom panel shows the probability (%) of fading events lower than –15 dB as a function of $S_4$, for the same sites.

Inspired by the performance of the α-µ model, another two-parameter distribution κ-µ model, proposed by Yacoub (2007b), was applied by Moraes *et al.* (2019) for ionospheric scintillation characterization. The results from this model were promising, presenting a performance almost as good as the α-µ model. Additionally, the κ-µ model showed very interesting results for GNSS signals under multipath fading due to urban environments, as presented by Lima Filho and Moraes (2021).

Two studies presented detailed assessments of the fading characteristics of the modernized signals. Salles *et al.* (2021a) provided empirical probability distributions of scintillation occurrence, average fading rate and durations at different Brazilian locations. The results confirmed the results by Moraes *et al.* (2018b), indicating that greater probabilities of strong scintillation occurrences are expected for the modernized L2C and L5 signals. In particular, the L5 signal reached average fade durations significantly longer than those for the other signals. A concerning result was the fading rate of the L5 signal, which reached up to five times more events than those observed at the traditional L1 band. The analysis also found that the average fade duration decreases at a rate equal to 0.6 s per 3 dB within the range from –6 to –15 dB. Complementing the above studies, Salles *et al.* (2021b) also showed that the L5 and L2C signal fades are deeper than those of the L1 GPS signal. The analysis showed that the deepest fading observed at Presidente Prudente (22.12°S, 51.40°W, geomagnetic latitude 16.01° S), considering 1-min records with $S_4(L1) \approx 0.6$, is typically –11 dB deeper on the L2C and L5 signals, when compared with the corresponding one on the L1 signal. Figure 9 shows the empirical probability of fading events deeper than –15 dB, as a function of $S_4$ at the L1 signal, for different sites characterized in Table 2.



Source: Elaborated by the authors.

**Figure 9.** Empirical probability, in percentage, of fading events deeper than –15 dB as a function of $S_4$ at the L1 signal for the three frequencies and four sites showing the L5 signals with higher probabilities.

Koulouri *et al.* (2020) used GNSS data during nighttime hours to describe scintillation effects on positioning accuracy. The authors proposed the concept of weighted position dilution of precision (WPDOP), which consists of allocating weights to satellite links, considering the ionospheric scintillation for each specific channel. That is, by tailoring weighted functions based on the geometry of the satellite-receiver path, as well as the respective scintillation measurements. This approach allowed the construction of ionospheric risk maps for GNSS users, showing the areas more susceptible to scintillation.

## GNSS Positioning Techniques with Emphasis on New Signals

In this project, a series of advances were proposed to improve positioning in low latitude regions. The first methodology estimated highly precise TEC values to obtain accurate solutions for geodetic positioning applications. The TEC accuracy was evaluated in terms of the PPP for a single frequency in the kinematic mode that reached one-centimeter accuracy similar to two-frequency PPP

(Prol *et al.* 2018c) and showed a 74% improvement over the same positioning technique using GIMs. A global study was performed using PPP Real-Time Kinematic (PPP-RTK) method to improve State Space Representation (SSR) modeling of ionospheric effects on positioning (Oliveira Junior *et al.* 2020), where an estimation of the receiver hardware biases based on ionospheric observables was successfully implemented. This methodology provided ionospheric delays with better accuracy (1~2 TECu).

Significant tests were carried out on the signal availability of new constellations, as well as their contribution to positioning in the São Paulo state region. The quality of the ambiguity solution, crucial for the high accuracy positioning and its rapid convergence, was analyzed (Silva *et al.* 2020). For example, Ma *et al.* (2021) implemented PPP procedures with integer ambiguity resolution in an airplane test, proofing the concept of improving the navigation accuracy in such application.

Successful ambiguity resolution is a key to precise positioning. In the ambiguity resolution process, the integer estimate can always be obtained, but it is essential to know whether it is correct or not, since erroneous estimates can deteriorate the final processing accuracy. Therefore, after obtaining the integer estimate, it is necessary to use validation tests that will inform on its quality. The Ratio Test is the most popular one in practical applications, but it cannot be the best choice, due to the failure rate for the application. To solve this problem, a more flexible approach, known as the Fixed Failure Ratio Test (FF-RT) was introduced. Silva *et al.* (2020) analyzed the performance of these two validation tests on the ambiguity resolution process. The results showed a better performance of the FF-RT test when compared to the Ratio Test, with the latter having a fixed ambiguity percentage of 47% and 31% in periods of weak and strong ionospheric activity, respectively, while the former increased the corresponding percentages to 80% and 67%.

With triple-frequency GNSS observations, the positioning performance is expected to be significantly improved. Cycle slip detection and correction play an important role in RTK positioning. Since cycle slips should be processed at every epoch, a fast determination method is needed for RTK applications. Mendonça *et al.* (2021) proposed a modified threshold for triple-difference (TD) procedures, using the Turbo Edit method to determine and correct cycle slips for triple-frequency GNSS RTK. The proposed algorithm utilizes the mean and standard deviation of TD series data to determine cycle slips in each pair of satellites. Also, the method can estimate cycle slips on a specific frequency. The proposed method was tested using real and simulated data for short and long baselines located in the São Paulo state. The results show that the proposed method can determine cycle slips on short baselines with 100% accuracy. For long baselines, the accuracy was 64 % for cycle-slip detection and 95 % for correction. The proposed method had similar results to those of the TD traditional method, for short baselines. For long baselines, the TD traditional method obtained 31% and 49% in the detection and correction accuracies, respectively, while the proposed method percentages were twice their corresponding ones.

Prol *et al.* (2018c) observed that the single-frequency PPP solution can provide a similar accuracy to that of dual-frequency. The only requirement is a highly precise TEC estimation, to correct the ionospheric delay in the phase and code observation at the L1 frequency. Based on experimental analyses, they concluded that the DCB and the temporal variation of the ionospheric delay do not preclude the PPP solution when using highly precise TEC values. In fact, the principal challenge in obtaining highly accurate PPP solutions is related with the spatial interpolation of the slant TEC values. In this regard, it is suggested that new ionospheric models should be developed to perform better TEC spatial interpolation.

Caldeira *et al.* (2020) evaluated the magnitude of ionospheric scintillation in Brazil and the performance of PPP under its influence during the period of high solar activity of the current cycle (24), through the Spearman correlation analysis and the Wavelet periodogram. Three-year time series (2012 to 2014) of the $S_4$ index and three-dimensional Mean-Squared Error (3D MSE) recorded by three Brazilian stations with different ionospheric conditions were considered: Palmas (10.18°S 48.33°W, geomagnetic longitude 7.61°S, near the geomagnetic equator), Presidente Prudente (low-latitude region, under the EIA), and Porto Alegre (mid-latitude region). Thus, it was possible to evaluate the correlation between the accuracy of PPP using only the GPS C/A code and the $S_4$ index. Correlations of 53% and 51%, using the Spearman method, were obtained for the Palmas and Presidente Prudente series, respectively. In addition, considering the analysis of space-frequency in relation to time by the wavelet coherence method, a correlation exceeding 70% was noted during the period of greatest 3D MSE, during the spring and autumn equinox months.

When using single-frequency pseudorange observations in positioning, it is common to use empirical or semi-empirical models to account for the ionospheric delay. Klobuchar and NeQuick G models are respectively associated to GPS and Galileo

systems, which broadcast coefficients that describe the worldwide mean ionospheric behavior. Therefore, it is possible to estimate the ionospheric delay for any time and location and apply these corrections to the pseudorange observations. Using multi-GNSS (GPS and Galileo) standard point positioning (SPP), Setti Júnior *et al.* (2019) compared the performance of both models, highlighting their weaknesses and strengthens, considering two Brazilian stations at different magnetic latitudes, covering months of weak and strong ionospheric activity from 2013 to 2018. The results indicated a better performance of the NeQuick G model when compared to that by Klobuchar. While the Klobuchar model improved the positioning accuracy by 16% and 50% in periods of weak and strong ionospheric activity, respectively, the corresponding NeQuick G model improvements were 31% and 55%.

With Galileo and BeiDou reaching full constellation, the combination of different signals and systems, called multi-GNSS, is increasingly becoming the state-of-the-art in geodetic positioning. The review paper by Setti Júnior *et al.* (2020) discussed the multi-GNSS integration in different positioning methods, including the SPP, PPP, DGNSS, RTK, Network-RTK (NRTK), and PPP-RTK. Some trends and challenges are also discussed, such as the stochastic modeling of different signals, use of low-cost receivers for high-accuracy positioning, atmospheric modeling using GNSS networks, and the use of GNSS for air navigation. A comparison of multi-GNSS (GPS, GLONASS, Galileo, and BeiDou) and GPS-only positioning is also described. Their results show that the integration of these systems can improve the positioning accuracy up to 44%.

Jerez and Alves (2020) also assessed the ionospheric regional and seasonal influence on the GNSS positioning over the Brazilian territory, using single and dual-frequency data (30-min and 4-h data) from three GNSS stations in regions with distinct ionospheric behavior. Precise point positioning results indicated the regional influence, with larger and sparser errors from the station located under the EIA, mainly considering data from October (seasonal influence). The use of GPS and GLONASS data was also evaluated, considering all configurations tested with 30-min data, and led to smaller errors in 97.35% of the cases when compared to autonomous GPS, which provided a mean improvement of about 60 cm, corresponding to 30%. Results and additional ionospheric scintillation indices ($S_4$ and $\sigma_\phi$) of PPP were also used in the study considering multivariate analysis techniques by Jerez *et al.* (2019). The applied strategies confirmed the regional and seasonal influence of the ionosphere on the positioning error, using techniques such as clustering and correspondence analysis. It was also confirmed the similar influence of the ionosphere in GPS and GLONASS data.

With the main goal of developing an ionospheric model capable of performing accurate spatial interpolation of TEC in the Brazilian area, thus providing better results in single-frequency PPP, Prol *et al.* (2019b) built a tomography algorithm that models the three-dimensional distribution of the electron density based on GNSS TEC and GPS radio-occultation measurements. The developed ionospheric tomography procedure was further validated through comparisons with ionosonde electron density, GPS TEC, and single-frequency PPP results. They obtained improvements of 31% for the F-layer peak height (hmF2) and 24% for the critical frequency (foF2), in comparison with estimations from the International Reference Ionosphere (IRI) model. In addition, improvements of 59% in TEC and 31% in the single-frequency PPP were obtained, when compared with one of the most accurate IGS GIMs, named Universitat Politècnica de Catalunya's Rapid GIM (UQRG). This confirms the capabilities of ionospheric tomography to improve the most recent geodetic techniques for GNSS positioning.

## GNSS Receiver Performance and Improvements under Scintillation Effects

Phase and amplitude scintillation can seriously affect receiver performance, depending on its severity. Ionospheric scintillation affects the code and phase tracking loops, causing receivers to provide degraded observables. Furthermore, the stressed loops can still lead to losses of lock. All these effects are undesirable for positioning users, due to performance degradation, which can even prevent the receiver from operating, thus totally losing the positioning capability. Figure 10 shows one example of PLL carrier tracking loop errors under scintillation effects. It is seen that the PLL phase errors substantially increase when fading events occur. Such events can result in cycle slips and losses of lock. This section reports on the advances achieved in the framework of the INCT project, with respect to: (1) receiver performance verification; and (2) the application of statistical signal processing techniques to reduce scintillation effects on the receiver performance.
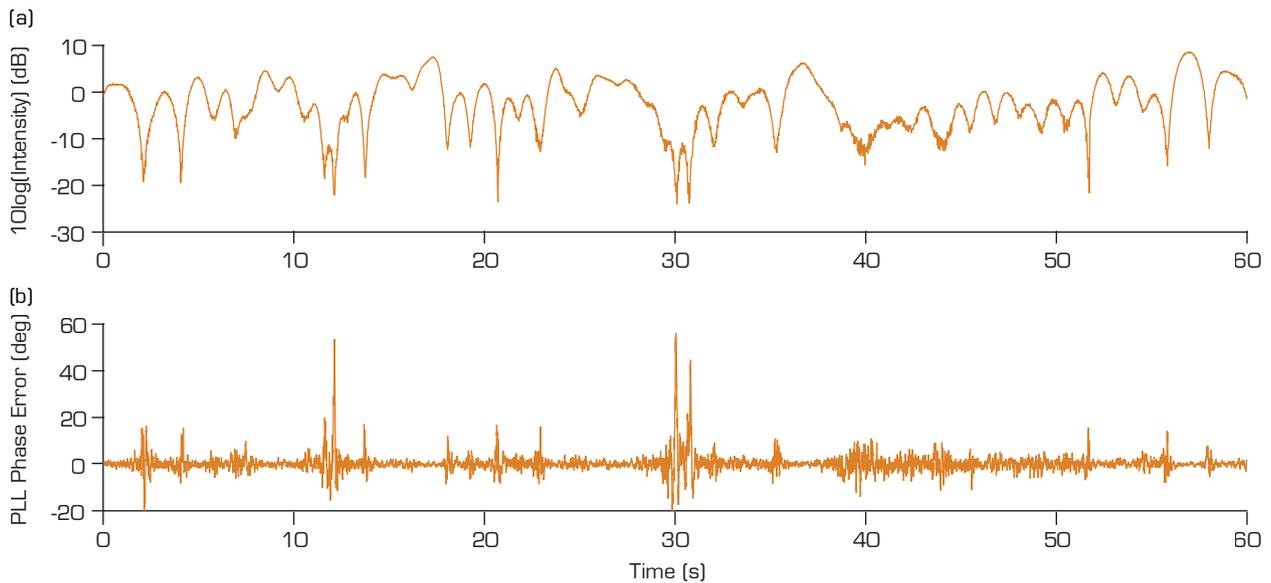
Source: Elaborated by the authors.

**Figure 10.** (a) Example of amplitude scintillation record with $S_4$ = 1.13. (b) corresponding PLL phase error, showing increases in loop estimation errors during deep-fading events.

A comparative analysis involving six different GNSS receiver models commonly used by the scientific community to study ionospheric irregularities was performed by de Paula *et al.* (2020). Using field data from two nights, this research demonstrated that different receiver models, with different hardware architecture and manufacturers, are able to provide similar $S_4$ estimates. Figure 11 shows the good agreement between the $S_4$ values estimated by five distinct receivers during the night 20 February 2013 at São José dos Campos. This result confirms that different measurement sources can be used together for works and studies on the characterization of ionospheric irregularities, as well as for the development of techniques to reduce scintillation effects on GNSS receivers.
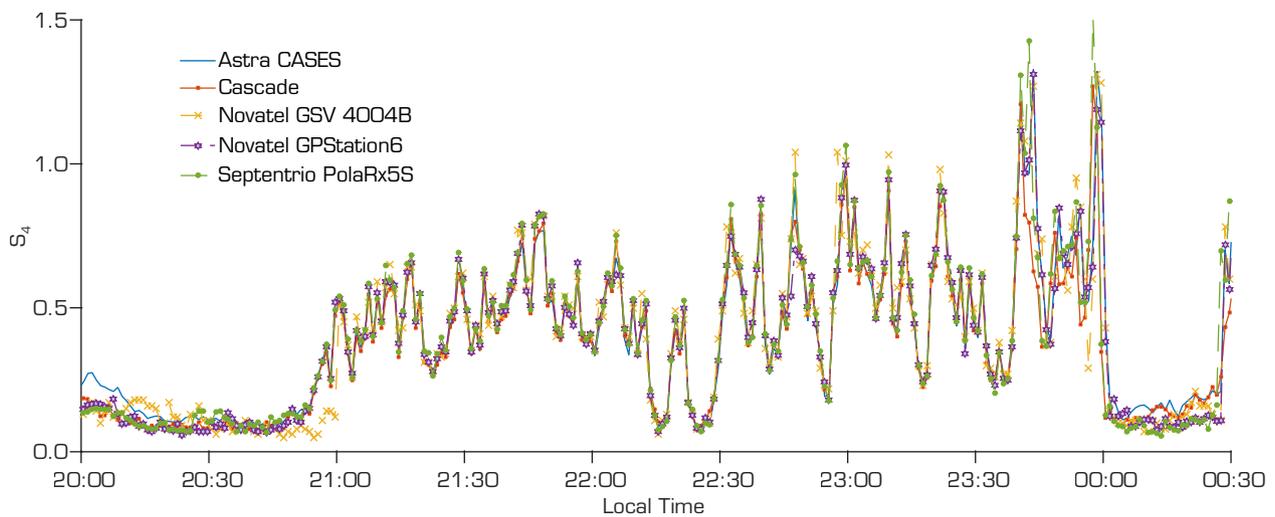


Source: Adapted from de Paula *et al.* (2020).

**Figure 11.** Scintillation index $S_4$ estimated by five different monitors for the night 20 February 2013 at São José dos Campos.

Vani *et al.* (2021) and Rodrigues and Moraes (2019) promoted the development of low-cost scintillation monitors. Such receivers, due to this characteristic, could be distributed in large-scale arrays for macroscopic ionospheric studies. This type of system is being used by undergraduate students in IFSP, for example, to learn concepts of hardware and software programming, satellite navigation, radio propagation and ionospheric physics, thus promoting scientific knowledge in different fields. Figure 12a shows the prototype of the low-cost scintillation monitor model Ionik. Figure 12b displays one example of a corresponding GPS signal under the influence of ionospheric scintillation. Figure 12c presents the estimated $S_4$ index based on the low-cost instrumentation, in comparison to the same index provided by the Septentrio PolaRx5S scintillation monitor. The comparison between the S4 indices shows a nice agreement between the results, supporting the use of this type of monitor for ionospheric studies. This example was recorded for PRN14 on 08 December 2016 at INPE's headquarters (São José dos Campos).
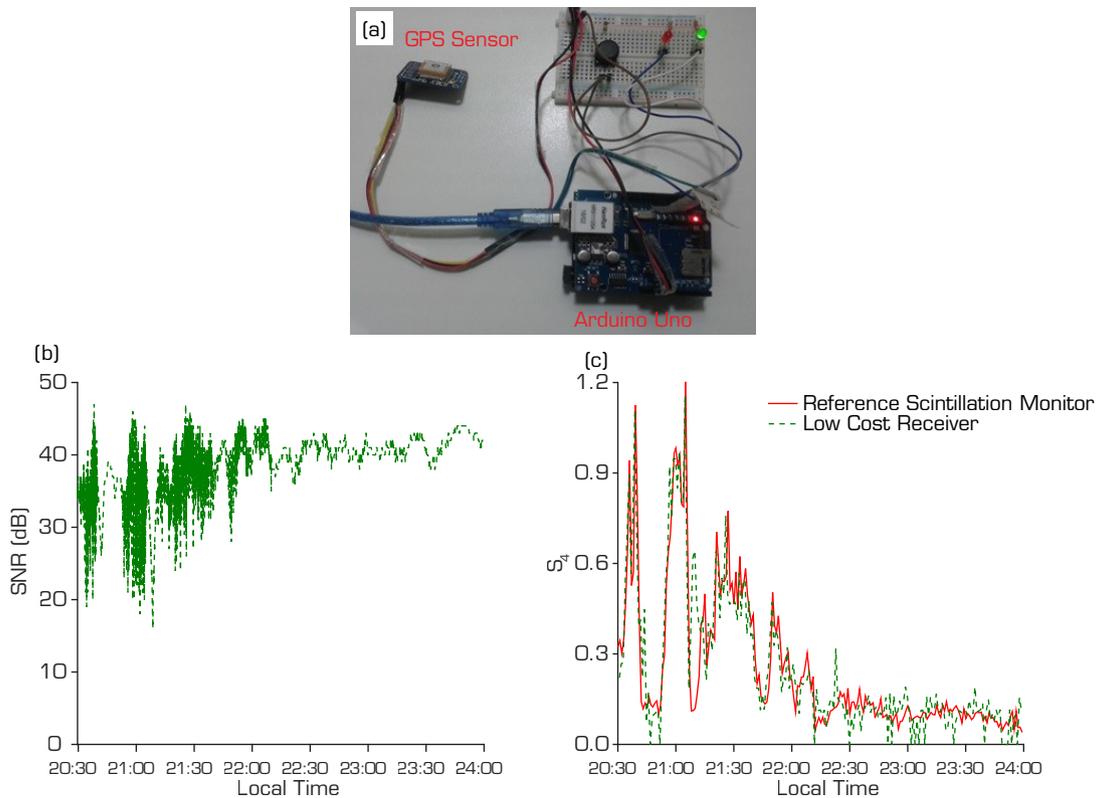


Source: Adapted from de Vani *et al.* (2021).

**Figure 12.** (a) Prototype of the scintillation monitor model Ionik; (b) Received GPS signal for PRN14 during 08 December 2016 at São José dos Campos; (c) Comparison between $S_4$ values estimated by the reference Septentrio PolaRx5S scintillation monitor and the ones acquired by the Ionik prototype.

Portella *et al.* (2021) tested the phase-locked loop (PLL) performance under different scintillation patterns and strengths. The work aimed at verifying which configuration (in terms of the PLL bandwidth) would be more tolerant to scintillation, according to each scenario. Using synthetic scintillation generator based on work by Humphreys *et al.* (2009), the $S_4$ and decorrelation time parameters were varied and tested for different bandwidth. The total occurrence of cycle slips was computed and the results showed that, for more intense scintillation environments, a wider bandwidth (15 Hz) is recommended, while narrower values are more suitable to weak scintillation. The work by Portella *et al.* (2021) also recorded the fading depth during cycle slip occurrences and how the bandwidth can make the receiver more tolerant to these events. Figure 13 shows the probability of cycle slip according to fading depth for two different scenarios. Another point highlighted in this research is that fades deeper than –15 dB typically lead to cycle slip occurrences, thus becoming an empirical threshold for receiver operation.

Another research developed in the framework of the INCT was reported by Veettil *et al.* (2020), who proposed a method for mitigating scintillation effects on PPP. They used a least squares (LSQ) stochastic model, where the variance of the tracking errors was applied as a weight. The variance was estimated with basis on the model by Moraes *et al.* (2014b), which employs the α-μ distribution. The results from this approach demonstrated improvements in the 3D positioning error up to 75%, which shows that this is a promising solution for users operating under the critical effects of strong scintillation.
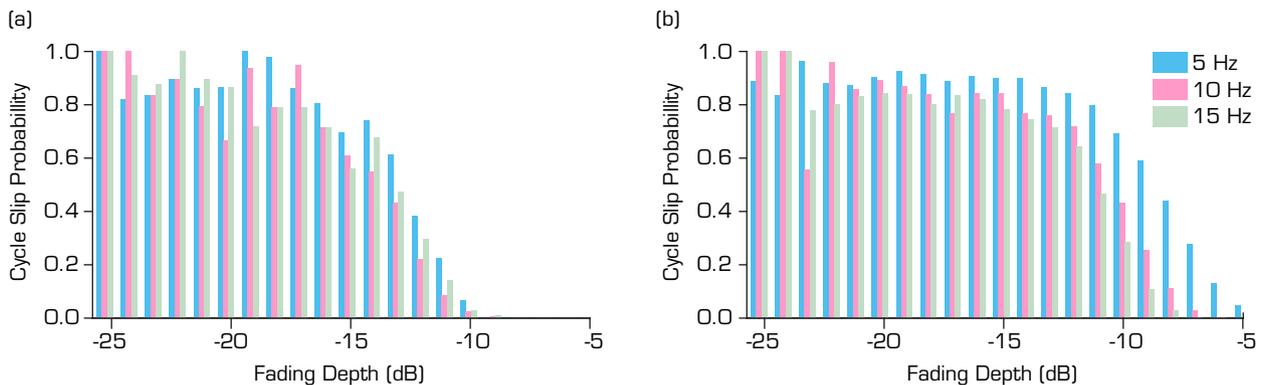


Source: Elaborated by the authors.

**Figure 13.** Empirical probability of cycle slip as a function of fading depth. (a) $S_4 = 0.8$ and $\tau_0 = 0.9$ s. (b) $S_4 = 0.9$ and $\tau_0 = 0.2$ s.

Vani *et al.* (2019) proposed a new approach, based mainly on the modification of the stochastic and functional modeling of GNSS observables, to attenuate scintillation effects on positioning. Such approach estimates an error component due to scintillation in the GNSS observable, named 'dScint' component. Experiments were carried out in the PPP context, with promising results. The proposed approach has the potential for implementation in any GNSS receiver, since the internal intensity and phase parameters are implicit in its tracking loops. The results from this method showed accuracy improvements up to 80%.

## CONCLUSIONS

The use of GNSS in air navigation is a worldwide reality. This dependence suggested the need to understand how the ionospheric environment can affect this class of users in equatorial and low latitudes regions. This work reported a series of progresses that have been achieved in this context. It is worth mentioning that, during this research, several students were trained on topics related to the INCT project. More than 28 master dissertations and 7 doctoral theses were generated.

There are still many open points that need to be researched and it is planned that the following list of studies will be developed in the course of this project:

- Start the development of a model that provides the probability of the occurrence of ionospheric scintillation above a risk level, when landing an aircraft;
- Evaluate the performance of a multifrequency GBAS in Brazil, in terms of accuracy, integrity and availability, using data from the L1, L2 and L5 carriers of the GPS, GLONASS and Galileo satellites. The station-pair method can be used in these studies, with one station representing a virtual GBAS station and the other a static virtual aircraft;
- In the next stage of the GBAS simulations using PEGASUS, the use of INCT GNSS NavAer Network stations will be resumed as one of the basic structures of the project. EUROCONTROL has made some indications of receiver configurations and simulations that can minimize GNSS station biases. The use of these stations will make it possible to

evaluate the performance of a Multifrequency/Multiconstellation GBAS (MF/MC GBAS) based on the use of Galileo's L1/L5 and E1/E5b observations. In addition, the modalities of GAST D and F services will be evaluated. These studies will be aided by the application of already recorded scintillation events to GNSS Spirent signal simulators. The outputs from these simulations will be used to evaluate the signal acquisition performance of several monitors under different scintillation situations;

- Expand the study of solar flare and Solar Radio Burst (SRB) effects on GNSS positioning;
- Additional investigations on the use of experimental or simulated data in a kinematic mode should be carried out, aiming at describing and improving GNSS receiver performances under scintillation;
- Most tests that have been carried out to date have been based on data collected by static monitoring GNSS receivers. This type of collection provides support for the investigation of models and improvements to mitigate scintillation effects on positioning. For applications with kinematic data (for example, associated with air navigation), greater challenges are expected. Indeed, the displacement of the receiver antenna makes it difficult to estimate several parameters, and especially those related with the phase observability of the carrier wave. In addition, the tests were based on standard settings applied to each receiver. With the use of a GNSS simulator, new tests assuming different internal configurations can be performed;
- Seek improvements in the quality control of the adjustment in the model of estimation of instrumental trends from ionospheric delays provided by the application of PPP-RTK techniques to data from reference stations;
- Include data from other constellations (such as GLONASS and Galileo) in the PPP method developed at Unesp with basis on GPS data;
- Include the NeQuick ionosphere model into the Unesp online PPS method;
- Estimation of TEC with precision better than 1 TECu using the PPP method with solution of the ambiguities and
- Implement the SPP using data from Smart Phones.

The following studies will also be continued: Single-frequency TEC estimation for detecting EPB aiming at developing a new positioning concept for aircraft and a more reliable source of information, when compared to a geometry-free combination, of dual frequencies; improve the calculation of EPB drift velocities from GNSS observations; investigate the impact of new signals and multi-GNSS positioning for ambiguity solution and PPP applications; and Include SSR modeling of ionosphere effects for PPP-RTK applications.


## AUTHORS' CONTRIBUTION

**Conceptualization:** Monico JFG, Moraes AO, Costa E, de Paula ER; **Methodology:** Monico JFG, De Paula ER, Moraes AO, Costa E, Shimabukuro MH, Alves DBM, Souza JR, Camargo PO, Prol FS, Vani BC, Pereira VSA, Oliveira Junior PS, Tsuchiya I, Aguiar CR; **Investigation:** Monico JFG, De Paula ER, Moraes AO, Costa E, Shimabukuro MH, Alves DBM, Souza JR, Camargo PO, Prol FS, Vani BC, Pereira VSA, Oliveira Junior PS, Tsuchiya I, Aguiar CR; **Writing – Original Draft:** Monico JFG, Costa E, Moraes AO, Marra Alves DB, de Souza JR, Prol FS, Pereira VSA; **Writing – Review and Editing:** Monico JFG, Costa E., de Paula ER; **Funding Acquisition:** Monico JFG, de Paula ER; **Resources:** Tyshushia I, Vani BC, Pereira VSA; **Supervision:** Monico JFG, de Paula ER, Moraes AO.


## DATA AVAILABILITY STATEMENT

Most of the raw data used in this paper are available to be downloaded by request through the "ISMR Query Tool" website: ismrquerytool.fct.unesp.br/ that belongs to GNSS NavAer project and from Rede Brasileira de Monitoramento Contínuio (RBMC) that belongs to Fundação Instituto Brasileiro de Geografia e Estatística (IBGE) which are free available. Estudo e Monitoramento Brasileiro do Clima Espacial/ INPE (EMBRACE) also provided data, most of them available on-line at http://www2.inpe.br/climaespacial/portal/pt/. The data acquired in the field tests with the low-cost experimental scintillation monitor (Figure 12) can be found in https://zenodo.org/record/6376121#.YjoSV_dv81k.

# FUNDING

# ACKNOWLEDGEMENTS

# REFERENCES

Abdu MA, Batista IS, Carrasco AJ, Brum CGM (2005) South Atlantic magnetic anomaly ionization: A review and a new focus on electrodynamic effects in the equatorial ionosphere. J Atmos Sol-Terr Phys 67(17-18):1643-1657. https://doi.org/10.1016/j.jastp.2005.01.014

Affonso BJ, Moraes AO, Sousasantos J, Marini-Pereira L, Pullen S (2022) Strong ionospheric spatial gradient events induced by signal propagation paths aligned with equatorial plasma bubbles. IEEE Trans Aerosp Electron Syst. https://doi.org/10.1109/TAES.2022.3144622

Bravo MA, Batista IS, Souza JR, Foppiano AJ (2019) Ionospheric response to disturbed winds during the 29 October 2003 geomagnetic storm in the Brazilian sector. J Geophys Res Space Phys 124(11):9405-9419. https://doi.org/10.1029/2019JA027187

Bravo MA, Martínez-Ledesma M, Foppiano A, Urra B, Ovalle E, Villalobos C, Souza J, Carrasco E, Muñoz P, Tamblay L, Vega-Jorquera P, Marín J, Pacheco R, Rojo E, Leiva R, Stepanova M (2020) First report of an eclipse from Chilean ionosonde observations: Comparison with total electron content estimations and the modeled maximum electron concentration and its height. J Geophys Res https://doi.org/10.1029/2020JA027923

Caldeira MCO, Caldeira CRT, Cereja SSA, Alves DBM, Aguiar CRD (2020) Evaluation of the GNSS positioning performance under influence of the ionospheric scintillation. Bol Ciênc Geod 26(3):e2020014. https://doi.org/10.1590/s1982-21702020000300014

Chapagain NP (2011) Dynamics of equatorial spread *F* using ground-based optical and radar measurements (doctoral dissertation). Logan: Utah State University.

Coleman TF, Li Y (1994) On the convergence of interior-reflective Newton methods for nonlinear minimization subject to bounds. Math Program 67:189-224. https://doi.org/10.1007/BF01582221

Datta-Barua S, Lee J, Pullen S, Luo M, Ene A, Qiu D, Zhang G, Enge, P. (2010) Ionospheric threat parameterization for local area global-positioning-system-based aircraft landing systems. J Aircr 47(4):1141-1151. https://doi.org/10.2514/1.46719

De Paula ER, Oliveira CBA, Caton RG, Negreti PM, Batista IS, Martinon ARF, Cunha Neto A, Abdu MA, Monico JFG, Sousasantos J, *et al.* (2019). Ionospheric irregularity behavior during the September 6–10, 2017 magnetic storm over Brazilian equatorial–low latitudes. Earth Planets Space 71:42. https://doi.org/10.1186/s40623-019-1020-z

De Paula ER, Martinon ARF, Moraes AO, Carrano C, Cunha Neto A, Doherty P, Groves DK, Valladares CE, Crowley G, Azeem I, *et al.* (2020) Performance of 6 different global navigation satellite system receivers at low latitude under moderate and strong scintillation. Earth Space Sci 8(2):e2020EA001314. https://doi.org/10.1029/2020EA001314.

Espejo TMS (2020) Simulation of equatorial and low-latitude ionospheric effects on the ground-based augmentation system (GBAS) (doctoral dissertation). Rio de Janeiro: Pontifícia Universidade Católica do Rio de Janeiro.

Humphreys TE, Psiaki ML, Hinks JC, O'Hanlon B, Kintner PM (2009) Simulating ionosphere-induced scintillation for testing GPS receiver phase tracking loops. IEEE J. Sel. Top. Signal Process 3(4):707-715. https://doi.org/10.1109/JSTSP.2009.2024130

Jerez GO, Alves DBM (2020) Assessment of GPS/GLONASS point positioning in Brazilian regions with distinct ionospheric behavior. Bol Ciênc Geod 26(2):e2020010. https://doi.org/10.1590/s1982-21702020000200010

Jerez GO, Alves DBM, Tachibana VM (2019) Multivariate analysis of combined GPS/GLONASS point positioning performance in Brazilian regions under different ionospheric conditions. J Atmos Sol Terr Phys 187:1-9. https://doi.org/10.1016/j.jastp.2019.03.003

Jerez GO, Hernández-Pajares M, Prol FS, Alves DBM, Monico JFG (2020) Assessment of Global Ionospheric Maps Performance by Means of Ionosonde Data. Remote Sens 12(20):3452. https://doi.org/10.3390/rs12203452

Jesus R, Batista IS, Takahashi H, Paula ER, Barros D, Figueiredo CAOB, Abreu AJ, Jonah OF, Fagundes PR, Venkatesh K (2020) Morphological features of ionospheric scintillations during high solar activity using GPS observations over the South American sector. J Geophys Res Space Phys 125(3). https://doi.org/10.1029/2019JA027441

Kim M, Choi Y, Jun HS, Lee J (2015) GBAS ionospheric threat model assessment for category I operation in the Korean region. GPS Solut 19:443-456. https://doi.org/10.1007/s10291-014-0404-6

Klipp T, Petry A, Souza JR, Falcao GS, Velho HF, Paula ER, Antreich F, Hoque M, Kriegel M, Berdermann J (2019) Evaluation of ionospheric models for Central and South Americas. Adv Space Res 64(10):2125-2136. https://doi.org/10.1016/j.asr.2019.09.005

Klipp TDS, Petry A, Souza JRD., Paula ERD, Falcão GS, Velho, HFC (2020) Ionosonde total electron content evaluation using International Global Navigation Satellite System Service data. Ann Geophys 38(2):347-357. https://doi.org/10.5194/angeo-38-347-2020

Koulouri A, Smith ND, Vani BC, Rimpiläinen V, Astin I, Forte B (2020) Methodology to estimate ionospheric scintillation risk maps and their contribution to position dilution of precision on the ground. J Geod 94:22. https://doi.org/10.1007/s00190-020-01344-0

Lee J, Pullen S, Datta-Barua S, Enge P (2007) Assessment of ionosphere spatial decorrelation for global positioning system-based aircraft landing systems. J Aircr 44(5):1662-1669. https://doi.org/10.2514/1.28199

Lima Filho VC, Moraes A (2021) Modeling multifrequency GPS multipath fading in land vehicle environments. GPS Solut 25:3. https://doi.org/10.1007/s10291-020-01040-8

Ma H, Verhagen S, Psychas D, Monico JFG, Marques HA (2021) Flight-test evaluation of integer ambiguity resolution enabled PPP. J Surv Eng 147(3):04021013. https://doi.org/10.1061/(ASCE)SU.1943-5428.0000367

Makela JJ, Vadas SL, Muryanto R, Duly T, Crowley G (2010) Periodic spacing between consecutive equatorial plasma bubbles. Geophys Res Lett 37(14):L14103. https://doi.org/10.1029/2010GL043968

Marini-Pereira L, Lourenço LFD, Sousasantos J, Moraes AO, Pullen S (2020) Regional ionospheric delay mapping for low-latitude environments. Radio Sci 55(12):e2020RS007158. https://doi.org/10.1029/2020RS007158

Marini-Pereira L, Oliveira K, Salles LA, Moraes AO, Paula ER, Muella MTAH, Perrella WJ (2019) On the field validation of α-μ fading coefficients estimator based on the autocorrelation function for ionospheric amplitude scintillation. Adv Space Res 64(10):2176-2187. https://doi.org/10.1016/j.asr.2019.06.012

Marini-Pereira L, Pullen S, Moraes AO, Sousasantos J (2021a) Ground-based augmentation systems operation in low latitudes-Part 1: Challenges, mitigations, and future prospects. J Aerosp Technol Manag 13:e4621. https://doi.org/10.1590/jatm.v13.1236

Marini-Pereira L, Pullen SP, Moraes A (2021b) Reexamining low-latitude ionospheric error bounds: An SBAS approach for Brazil. IEEE Trans Aerosp Electron Syst 57(1):674-689. https://doi.org/10.1109/TAES.2020.3029623

Martínez-Ledesma M, Bravo M, Urra B, Souza J, Foppiano A (2020) Prediction of the ionospheric response to the 14 December 2020 total solar eclipse using SUPIM-INPE. J. Geophys. Res. Space Phys 125(11): e2020JA028625. https://doi.org/10.1029/2020JA028625

Mayer C, Belabbas B, Jakowski N, Meurer M, Dunkel W (2009) Ionosphere threat space model assessment for GBAS. Proceedings of the 22nd International Technical Meeting of The Satellite Division of the Institute of Navigation (ION GNSS 2009); 2009 Sep 22-25; Savannah, GA. Virgínia: ION. p. 1091-1099.

Mendonça CHC, Alves DBM, Silva CM (2021) Melhoria no limiar de detecção de perda de ciclos para o método das TD no posicionamento relativo. Rev Bras Cartogr 73(1):106-118. https://doi.org/10.14393/rbcv73n1-49588

Moraes AO, Costa E, Paula ER, Perrella WJ, Monico JFG (2014b) Extended ionospheric amplitude scintillation model for GPS receivers. Radio Sci 49(5):315-329. https://doi.org/10.1002/2013RS005307

Moraes AO, Paula ER, Muella MTAH, Perrella WJ (2014a) On the second order statistics for GPS ionospheric scintillation modeling. Radio Sci 49(2):94-105. https://doi.org/10.1002/2013RS005270

Moraes AO, Vani BC, Costa E, Abdu MA, Paula ER, Sousasantos J, Monico JFG, Forte B, Negreti PMS, Shimabukuro MH (2018a) GPS availability and positioning issues when the signal paths are aligned with ionospheric plasma bubbles. GPS Solut 22:95. https://doi.org/10.1007/s10291-018-0760-8

Moraes A, Sousasantos J, Paula ER, Cunha JJPP, Lima Filho VC, Vani BC (2019) Performance analysis of κ-μ distribution for Global Positioning System (GPS) L1 frequency-related ionospheric fading channels. J Space Weather Space Clim 9:A15. https://doi.org/10.1051/swsc/2019012

Moraes AO, Vani BC, Costa E, Sousasantos J, Abdu MA, Rodrigues F, Gladek YC, Oliveira CBA, Monico JFG (2018b) Ionospheric scintillation fading coefficients for the GPS L1, L2, and L5 frequencies. Radio Sci 53(9):1165-1174. https://doi.org/10.1029/2018RS006653

Oliveira CBA, Espejo TMS, Moraes A, Costa E, Sousasantos J, Lourenço LFD, Abdu M. A (2020) Analysis of plasma bubble signatures in total electron content maps of the low-latitude ionosphere: A simplified methodology. Surv Geophys 41:897-931. https://doi.org/10.1007/s10712-020-09584-7

Oliveira Junior PS, Monico JFG, Morel L (2020) Mitigation of receiver biases in ionospheric observables from PPP with ambiguity resolution. Adv Space Res 65(8):1941-1950. https://doi.org/10.1016/j.asr.2020.01.037

Pautet PD, Taylor MJ, Chapagain NP, Takahashi H, Medeiros AF, São Sabbas FT, Fritts DC (2009) Simultaneous observations of equatorial F-region plasma depletions over Brazil during the Spread F experiment (SpreadFEx). Ann Geophys 27:2371-2381. https://doi.org/10.5194/angeo-27-2371-2009

Pereira VAS, Monico JFG, Camargo PO (2021a) Detection of solar flare using IGS network stations: case study for September 6, 2017. Rev Bras Geom 9(2):103-119.

Pereira VAS, Monico JFG, Camargo PO (2021b) Estimation and analysis of protection levels for precise approach at Rio de Janeiro international airport using real time $\sigma_{VIG}$ for each GPS and GLONASS satellite. Bol Ciênc Geod 27(spe):e2021010. https://doi.org/10.1590/s1982-21702021000s00010

Portella IP, Moraes AO, Pinho MS, Sousasantos J, Rodrigues F (2021) Examining the tolerance of GNSS receiver phase tracking loop under the effects of severe ionospheric scintillation conditions based on its bandwidth. Radio Sci 56(6):e2020RS007160. https://doi.org/10.1029/2020RS007160

Prol FS, Camargo PO, Hernández-Pajares M, Muella MTAH (2019b) A new method for ionospheric tomography and its assessment by ionosonde electron density, GPS TEC, and single-frequency PPP. IEEE Trans Geosci Remote Sens 57(5):2571-2582. https://doi.org/10.1109/TGRS.2018.2874974

Prol FS, Camargo P, Monico JFG, Muella MTAH (2018c) Assessment of a TEC calibration procedure by single-frequency PPP. GPS Solut 22:35. https://doi.org/10.1007/s10291-018-0701-6

Prol FS, Hernández-Pajares M, Camargo PO, Muella MTAH (2018b) Spatial and temporal features of the topside ionospheric electron density by a new model based on GPS radio occultation data. J Geophys Res Space Phys 123(3):2104-2115. https://doi.org/10.1002/2017JA024936

Prol FS, Hernández-Pajares M, Muella MTAH, Camargo P (2018a) Tomographic imaging of ionospheric plasma bubbles based on GNSS and radio occultation measurements. Remote Sens 10(10):1529. https://doi.org/10.3390/rs10101529

Prol FS, Themens DR, Hernández-Pajares M, Camargo PO, Muella MTAH (2019a) Linear Vary-Chap topside electron density model with topside sounder and radio-occultation data. Surv Geophys 40:277-293. https://doi.org/10.1007/s10712-019-09521-3

Pullen S, Park YS, Enge P (2009) Impact and mitigation of ionospheric anomalies on ground-based augmentation of GNSS. Radio Sci 44(1):RS0A21. https://doi.org/10.1029/2008RS004084

Rodrigues FS, Moraes AO (2019) ScintPi: A low-cost, easy-to-build GPS ionospheric scintillation monitor for DASI studies of space weather, education, and citizen science initiatives. Earth Space Sci 6(8):1547-1560. https://doi.org/10.1029/2019EA000588

Salles LA, Moraes A, Vani B, Sousasantos J, Affonso BJ, Monico JFG (2021a) A deep fading assessment of the modernized $L_2C$ and $L_5$ signals for low-latitude regions. GPS Solut 25:122. https://doi.org/10.1007/s10291-021-01157-4

Salles LA, Vani BC, Moraes A, Costa E, Paula ER (2021b) Investigating ionospheric scintillation effects on multifrequency GPS signals. Surv Geophys 42:999-1025. https://doi.org/10.1007/s10712-021-09643-7

Santos AM, Batista IS, Sobral JHA, Brum CGM, Abdu MA, Souza JR (2020) Some differences in the dynamics of the intermediate descending layers observed during periods of maximum and minimum solar flux. J Geophys Res Space Phys 125(10):e2019JA027682. https://doi.org/10.1029/2019JA027682

Setti Júnior PDT, Alves DBM, Silva CM (2019) Klobuchar and Nequick G ionospheric models comparison for multi-GNSS single-frequency code point positioning in the Brazilian region. Bol Ciênc Geod 25(3):e2019016. https://doi.org/10.1590/s1982-21702019000300016

Setti Júnior PT, Silva CM, Oliveira Júnior PS, Alves DBM, Monico JFG (2020) Posicionamento multi-GNSS. Rev Bras Cartogr 72(Especial 50 anos):1200-1224. https://doi.org/10.14393/rbcv72nespecial50anos-56580

Silva ALA, Sousasantos J, Marini-Pereira L, Lourenço LFD, Moraes AO, Abdu MA (2021) Evaluation of the dusk and early nighttime Total Electron Content modeling over the eastern Brazilian region during a solar maximum period. Adv Space Res 67(5):1580-1598. https://doi.org/10.1016/j.asr.2020.12.015

Silva CM, Setti Júnior PS, Alves DBM, Souza EM (2020) GNSS ambiguity resolution with ratio and fixed failure ratio tests for long baseline network RTK under ionospheric activity. J Atmos Sol-Terr Phys 202:105256. https://doi.org/10.1016/j.jastp.2020.105256

Silva RP, Souza JR, Sobral JHA, Denardini CM, Borba. GL, Santos MAF (2019) Ionospheric plasma bubble zonal drift derived from total electron content measurements. Radio Sci 54(7)580-589. https://doi.org/10.1029/2018RS006727

Sousasantos J, Moraes AO, Sobral JHA, Muella MTAH, Paula ER, Paolini RS (2018) Climatology of the scintillation onset over southern Brazil. Ann Geophys 36(2):565-576). https://doi.org/10.5194/angeo-36-565-2018

Sousasantos J, Marini-Pereira L, Moraes AO, Pullen S (2021) Ground-based augmentation system operation in low latitudes-part 2: Space weather, ionospheric behavior and challenges. J Aerosp Technol Manag 13:e4821. https://doi.org/10.1590/jatm.v13.1237

Souza ALC, Camargo PDO (2019) Comparison of GNSS indices, ionosondes and all-sky imagers in monitoring the ionosphere in Brazil during quiet and disturbed days. Bol Ciênc Geod 25(SPE):e2019s005. https://doi.org/10.1590/s1982-21702019000s00005

Souza ALC, Camargo PDO, Muella M, Tardelli-Coelho F (2021) Drift velocity estimation of ionospheric bubbles using GNSS observations. Radio Sci 56(8):e2020RS007220. https://doi.org/10.1029/2020RS007220

Takahashi H, Taylor MJ, Pautet PD, Medeiros AF, Gobbi D, Wrasse CM, Fechine J, Abdu MA, Batista IS, Paula E, Sobral JHA, Arruda D, Vadas SL, Sabbas FS, Fritts DC (2009) Simultaneous observation of ionospheric plasma bubbles and mesospheric gravity waves during the SpreadFEx campaign. Ann Geophys 27:1477-1487. https://doi.org/10.5194/angeo-27-1477-2009

Vani BC, Forte B, Monico JFG, Skone S, Shimabukuro MH, Moraes AO, Portella IP, Marques HA (2019) A novel approach to improve GNSS Precise Point Positioning during strong ionospheric scintillation: Theory and demonstration. IEEE Trans Veh Technol 68(5):4391-4403. https://doi.org/10.1109/TVT.2019.2903988

Vani BC, Moraes A, Salles LA, Breder VHF, Freitas MJS, Monico JFG, Paula ER (2021). Monitoring ionospheric scintillations with GNSS in South America: Scope, results, and challenges. In: Petropoulos GP, Srivastava PK, editors. GPS and GNSS Technology in Geosciences. Amsterdam: Elsevier. p. 255-280. https://doi.org/10.1016/B978-0-12-818617-6.00012-3

Vani BC, Shimabukuro MH, Monico JFG (2017) Visual exploration and analysis of ionospheric scintillation monitoring data: The ISMR query tool. Comput Geosci 104:125-134. https://doi.org/10.1016/j.cageo.2016.08.022

Veettil SV, Aquino M, Marques HA, Moraes A (2020) Mitigation of ionospheric scintillation effects on GNSS precise point positioning (PPP) at low latitudes. J Geod 94:15. https://doi.org/10.1007/s00190-020-01345-z

Yacoub MD (2007a) The $\alpha$-$\mu$ distribution: A physical fading model for the Stacy distribution. IEEE Trans Veh Technol 56(1):27–34. https://doi.org/10.1109/TVT.2006.883753

Yacoub MD (2007b) The $\kappa$-$\mu$ distribution and the $\eta$-$\mu$ distribution. IEEE Antennas Prop Mag 49(1):68-81. https://doi.org/10.1109/MAP.2007.370983